Image Texture Processing and Data Integration for Surface Pattern Discrimination

Derek R. Peddle and *Steven E. Franklin*
Department of Geography, The University of Calgary, Calgary, Alberta T2N 1N4, Canada

ABSTRACT: This study evaluates the increases in classification accuracy possible from satellite and airborne image texture processing and integration with ancillary topographic data for a moderate relief, boreal environment in Gros Morne National Park, eastern Canada. The texture measures angular second moment, entropy, and inverse difference moment were computed from spatial co-occurrence matrices in different orientations from SPOT multispectral linear array (MLA) and synthetic aperture radar (SAR) imagery. The general system of geomorphometry (elevation, slope, aspect, curvature, relief) was extracted from a co-registered digital elevation model (DEM). Stepwise and linear discriminant analyses were used to rank the relative information content of all variables and to ascertain classification accuracies for different combinations of variables. The analysis was applied to random samples of image data stratified by nine vegetation/land-cover classes determined from field work and aerial photointerpretation. The three variables containing the greatest relative discriminatory power were MLA band 2, SAR angular second moment, and elevation. Overall classification accuracies were as follows: SAR image alone: 36 percent; SAR with texture: 47 percent; DEM: 59 percent; geomorphometry: 69 percent; MLA image alone: 73 percent; MLA image and texture: 88 percent; MLA and geomorphometry: 94 percent; and MLA with texture and geomorphometry: 98 percent. The spatial co-occurrence matrices contain important textural information that improved the discrimination of classes with internal heterogeneity and structural/geomorphometric patterns. Greater improvements were obtained through data integration, and the highest accuracy achieved used a combined texture processing/integration approach with MLA and geomorphometric data. Optimization procedures which use *a priori* rank analysis and selective data processing in a two-stage classification are proposed to alleviate potential classifier problems associated with the increased number of variables being considered.

INTRODUCTION

IMAGE TEXTURE PROCESSING and ancillary data integration are two common approaches used to increase the accuracy of remote sensing classifications. Texture is an important discriminating characteristic of an image region (Curran, 1985, p. 204), and its use in digital image classification is based on the need to include pattern variability in the analysis (Weszka *et al.*, 1976). Common texture processing algorithms include spatial co-occurrence, second-order gray level statistics, autocorrelation functions, image transformations, and edge filter operators (Haralick, 1979). Texture analysis of spectral response has been used in many applications, including terrain analysis (Shih and Schowengerdt, 1983), forest mapping (Skidmore, 1989; Gordon and Philipson, 1986), environmental monitoring (Cross *et al.*, 1988), and in ecological studies (Saxon, 1984), while applications of radar texture can be found in forestry (Leckie, 1984; Lowry *et al.*, 1986), land use (Ulaby *et al.*, 1986), agriculture (Pultz and Brown, 1987), and sea ice differentiation (Gersen and Rosenfeld, 1975; Peddle, 1989).

Digital techniques to accomplish ancillary data integration are generally either deterministic or probabilistic (Hutchinson, 1982; Franklin, 1989). Examples which used remotely sensed spectral response and digital elevation models have been applied to forestry studies (Fleming and Hoffer, 1979; Cook *et al.*, 1989), terrain analysis (Franklin, 1987; Jones *et al.*, 1988; Frank, 1988) and wildlife management (Kenk and Yee, 1988). Studies that used radar and elevation data in forestry studies in mountainous areas include Lowry *et al.* (1986) and Teillet *et al.* (1985), among others.

This paper addresses the use of both techniques. Results are presented from a program of research in image texture processing and integration of ancillary topographic data in Gros Morne National Park, eastern Canada (see Figure 1). Earlier work in this boreal environment showed significant increases in classification accuracy using (1) a Landsat MSS image with ancillary elevation data (Franklin *et al.*, 1989); (2) Landsat MSS texture and geomorphometry (Franklin and Peddle, 1989); and (3) texture analysis of high resolution SPOT satellite imagery (Franklin and Peddle, 1990). In this study, additional work using airborne radar data and stepwise and linear discriminant procedures is described to reveal the relative information content of the spectral, radar, and topographic variables, and to determine optimal mapping combinations and processing strategies in a probabilistic classification of complex surface patterns in an area of diverse land cover and terrain.

Two main hypotheses are tested: (1) classification accuracy increases significantly when new variables processed from high resolution data are introduced, and (2) the integration of ancillary data sources provides new information that will improve the description and discrimination of ground classes.

With these hypotheses in mind, the following experiment was designed: (1) nine vegetation-community/land-cover classes were identified from field work and aerial photointerpretation; (2) co-registered data sets were prepared consisting of MLA and SAR imagery and a DEM; (3) image texture processing and geomorphometric algorithms were applied; (4) a random sample of pixels was generated for all variables within field-checked training sites; (5) all variables were ranked statistically according to their relative discriminatory power and non-redundant information content; and (6) linear discriminant analysis was used to determine individual and overall class accuracies for various data set combinations. In each case, the assessment is based on direct comparisons to known and established ground conditions observed in the field.

STUDY AREA

The study area is located on the west coast of the island of Newfoundland within the boundary of Gros Morne National Park (see Figure 1). The Park covers over 1800 square kilometres and includes at least six land regions: Coastal Plain, Piedmont Moraines, Long Range Mountain Frontal Slopes, Long Range Uplands, Southern Hills, and a Klippe Complex. The Long Range Mountains are the dominant topographic feature and are part of the Appalachian chain of mountains in eastern North America. The study area selected for analysis encompasses a diversity

PHOTOGRAMMETRIC ENGINEERING & REMOTE SENSING,
Vol. 57, No. 4, April 1991, pp. 413–420.

0099-1112/91/5704–413$03.00/0
©1991 American Society for Photogrammetry
and Remote Sensing

FIG. 1. Location of the study area, Gros Morne National Park, Newfoundland, Canada.

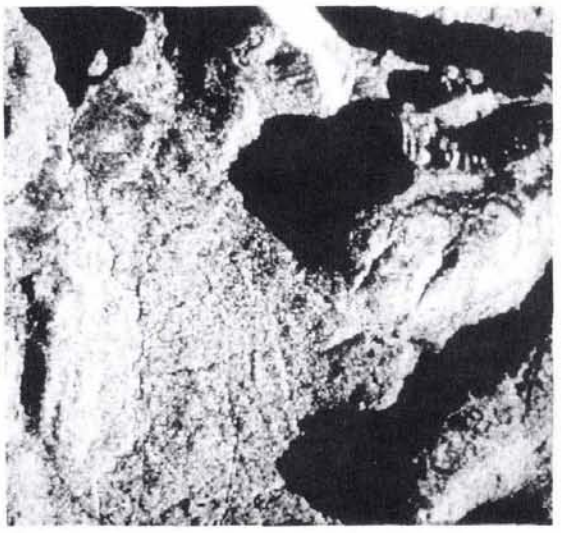

FIG. 2. Aerial synthetic aperture radar (SAR) image in plan perspective.

of vegetation communities and land forms and includes the full range of relief in the Park from sea level to the summit of Gros Morne Mountain (806 m above sea level). A complete description of the land regions and land systems of this area is provided in the Park Biophysical Resources Inventory (AAACL, 1975).

DATA ACQUISITION

A SPOT-1 multispectral linear array (MLA) high resolution visible (HRV) image was acquired on 17 August 1988 with an off-nadir viewing angle of 20.24 degrees west, solar elevation of 52.9 degrees, and solar azimuth of 164.7 degrees. This scene is cloud-free and without visible radiometric degradation. Airborne synthetic aperture radar (SAR) C-band imagery was acquired on 7 September 1988 in HH polarization, narrow swath mode at a spatial resolution of 6 m by The Canada Centre for Remote Sensing Convair 580 aircraft flying at an altitude of 6100 m. The digital elevation model (DEM) of Gros Morne National Park was created by digitizing contours from a mylar copy of the 1:100,000-scale topographic map of the area using a precision coordinate digitizer. A dense-grid 20-m DEM was produced after interpolation by an average distance-weighted vector to raster transformation routine (Davis, 1987) of the Surface II computer mapping system. All of the data sets were registered to the Universal Transverse Mercator (UTM) projection using standard geometric correction procedures with less than 0.5 pixel error.

A color composite of the SPOT MLA imagery is shown in Plate 1 as a three-dimensional perpective image visualization generated by draping a three-band enhancement over the DEM (see Hussey *et al.*, 1986). The SAR image is shown in plan view as a gray level image in Figure 2.

IMAGE PROCESSING

Texture processing of the MLA and SAR imagery was accomplished using the spatial co-occurrence algorithm proposed by Haralick *et al.* (1973) and implemented by Franklin and Peddle (1987). In that algorithm, relationships of adjacent gray tones are captured in spatial co-occurrence matrices for a specified orientation and window size from which a series of texture measures can be computed (see Haralick *et al.* (1973) and Weszka *et al.* (1976)).

Figure 3 illustrates the construction of the four directional spatial co-occurrence matrices for a 3 by 3 window from an example image normalized to four gray levels (0 to 3). Pairs of adjacent pixels are considered in orientation, and the normalized value of those pixels forms the index for incrementing an entry of the co-occurrence matrix. The final matrix for a given point location in the image contains the number of times each possible pair of pixel values occurred in the selected orientation within the specified neighbourhood surrounding that point.

In this study, three texture measures were used: angular second moment (ASM) — a measure of homogeneity; entropy — a measure of randomness; and inverse difference moment (IDM) — a measure of lack of variability. The formulae used to compute each measure from the spatial co-occurrence matrix at each point are as follows:

$$\text{angular second moment} = \sum_i \sum_j \left\{ \frac{P(i,j)}{R} \right\}^2 \tag{1}$$

$$\text{entropy} = -\sum_i \sum_j \left(\frac{P(i,j)}{R} \right) \log \left(\frac{P(i,j)}{R} \right) \tag{2}$$

$$\text{inverse difference moment} = \sum_i \sum_j \frac{1}{1 + (i-j)^2} \left(\frac{P(i,j)}{R} \right) \tag{3}$$

where P is the spatial co-occurrence matrix and R is the frequency normalization constant for the selected orientation.

Many texture features could be generated from each band using different texture measures, window sizes, orientations, and gray level ranges (see Haralick *et al.*, 1973). However, texture processing was curtailed in this study to one feature per band in order to minimize dimensionality problems associated with entering additional variables into a classifier. The texture processing options were selected with reference to an earlier study of MLA texture elsewhere in the Park (Franklin and Peddle, 1990). The following texture features were computed from the MLA image using an 11 by 11 window (220 m by 220 m on the ground): ASM of band 1 in the horizontal orientation, entropy of band 2 in the right diagonal orientation, and IDM of band 3 in the left diagonal orientation. The three MLA texture features are shown in color composite in Plate 2. From the single band SAR image, ASM, entropy, and IDM were computed at full

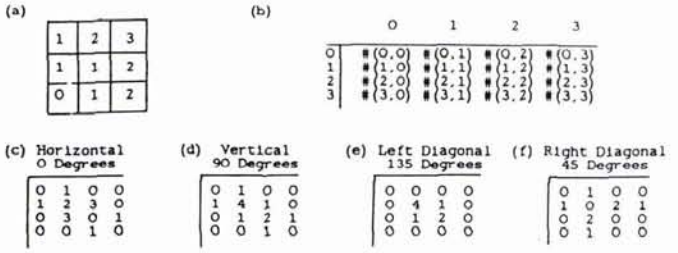

FIG. 3. (a) 3 by 3 window with gray tone range 0 to 3; (b) general form of any spatial co-occurrence matrix for window with gray tone range 0 to 3. $\#(i,j)$ represents number of times gray tones i and j were neighbors. (c) to (f) spatial co-occurrence matrices derived for four angular orientations.

image resolution in the horizontal, right diagonal, and left diagonal orientations, respectively, using a 37 by 37 window size (222 m by 222 m on the ground). The co-occurrence orientation in each case was based on an earlier study (Franklin and Peddle, 1989) where it was found that individual texture orientations resulted in higher class accuracies than averaged texture measures. The selection of window size (approximately 200 m by 200 m on the ground) was based on observations in the field, aerial reconnaissance, photointerpretation, and earlier tests and successful uses of texture to improve the classification of MLA imagery (Franklin and Peddle, 1990).

The general system of geomorphometry (Evans, 1972) was extracted from the DEM using the GEDEMON software package (Peddle and Franklin, 1990) to obtain measures of elevation, slope, aspect transformed to incidence (see Townshend, 1981), down slope convexity, cross slope convexity, and relief.

Both the texture analysis software, written in the C programming language (see Franklin and Peddle, 1987) and the FORTRAN GEDEMON software package (Peddle and Franklin, 1990) run on a VAX-11/750 computer under the VMS operating system. Those interested in obtaining a copy of either program are welcome to contact the authors.

FIELD CLASSIFICATION AND SAMPLING DESIGN

Field work and interpretation of the black-and-white aerial photography (see Figure 4) were used to find areas representative of nine vegetation-community/land-cover classes that are described in Table 1 and mapped in Figure 5. These classes are the basis for the vegetation maps analyzed by National Parks personnel in their biophysical inventory of the Park's resources. The stars in Figure 5 show the location of sites verified by field observations as representative of each class. These sites were located in the registered data sets on the image analysis system. A disproportional stratified random sample (Townshend, 1981) was generated consisting of 900 training and 900 test pixels (100 pixels per sample for each of the nine classes). The general rule of thumb is to have $100n$ pixels in a sample, where n is the number of variables (Swain and Davis, 1978). This rule is adhered to for all but five of the discriminant functions tested (i.e., those which use not more than nine variables — see Table 3) because it was not possible to visit enough representative sites in the field. In addition to this, several of our field sites were invalidated since they were located in radar shadow (see Figure 2). Therefore, the functions which test ten or more variables must be interpreted with caution.

DISCRIMINANT ANALYSIS RESULTS

Stepwise and linear discriminant analysis procedures (Cooley and Lohnes, 1971; Klecka, 1980) were used in the Statistical Analysis System (SAS Institute, 1985) to investigate the relative discriminatory power of all variables and to determine classification accuracies for different variable combinations.

Discriminant analysis was chosen as the method of implementing a classification because it has been shown to be less sensitive to the number of mapping variables and less affected by deviations from the normal (Gaussian) distribution compared to other classification techniques, such as maximum like-

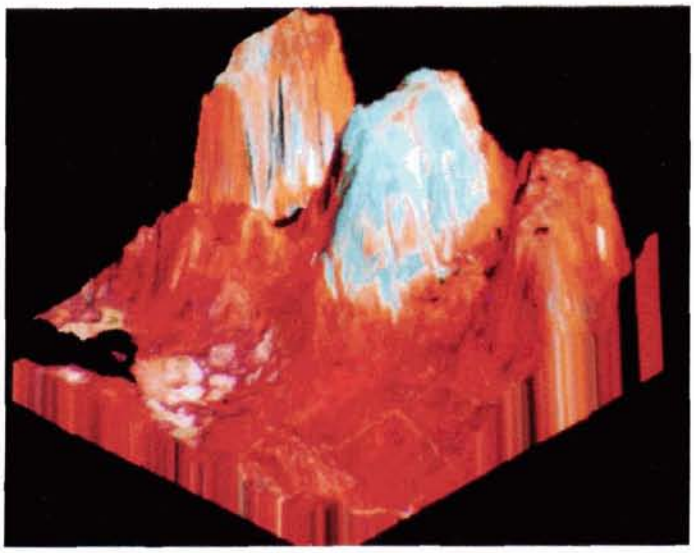

PLATE 1. SPOT MLA band 3, 2, 1 color composite draped over the DEM in perspective view. Viewing geometry 45 degrees off the horizon, looking northeast, with no vertical exaggeration.

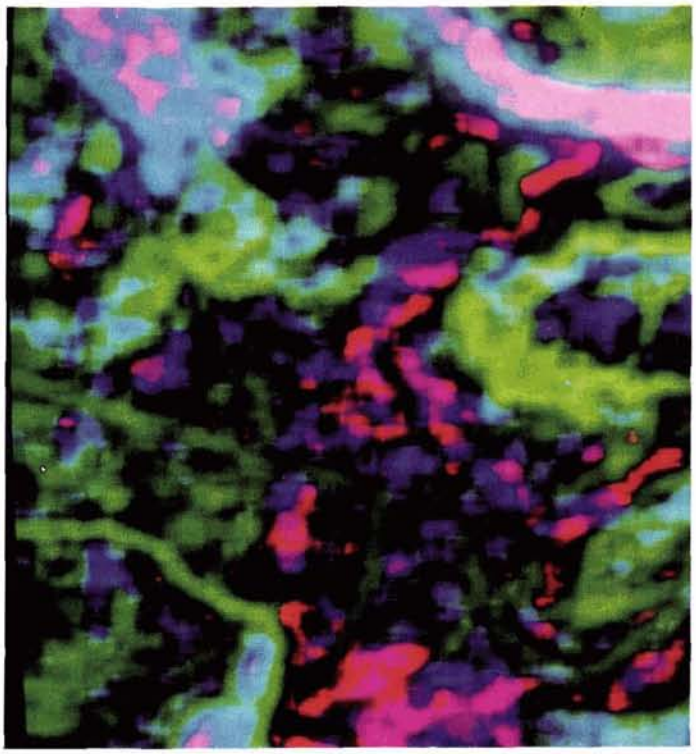

PLATE 2. Color composite of SPOT MLA texture features in plan view. ASM of band 1 shown in red, entropy of band 2 in green, and IDM of band 3 in blue.

FIG. 4. Reproduction of aerial photograph of the study area (original scale approximately 1:30,000).

TABLE 1. LAND-COVER CLASSES

Class	Description	Label in Figure 5
1	Heath, Scattered Black Spruce	HBs
2	Heath Barrens	HB
3	Water	
4	Nunatak—Exposed Serpentines	N
5	Spruce Shrub/Tuckamoor Plateau	TP
6	Black Spruce Forest	Bs
7	Balsam Fir Forest	BF
8	White Birch Forest	BW
9	Mixed Forest (BF,BW,Bs)	M

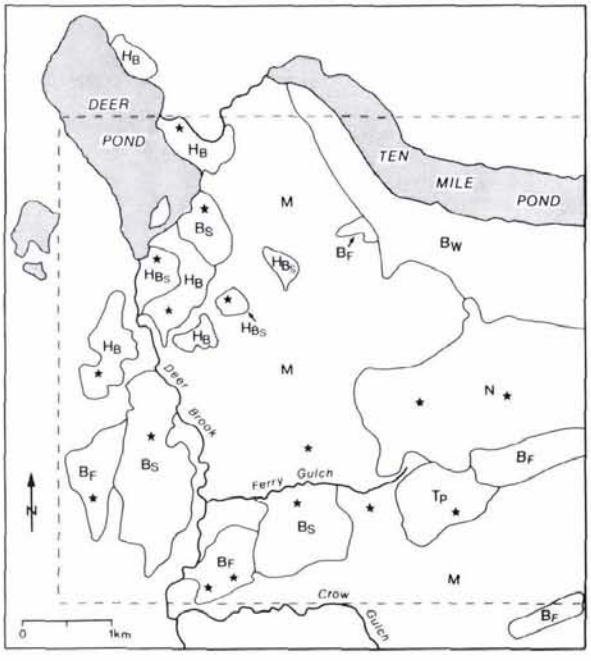

FIG. 5. Field classification map. Stars show the location of sampled training areas. Class labels in Table 1.

lihood (Tom and Miller, 1984). It is also important to note that classification accuracy is in part a function of the class structure used with respect to the spatial and radiometric precision of the data (Hutchinson, 1982).

RANKING OF VARIABLES

Stepwise discriminant analysis is a variable-selection technique whereby variables are entered into the model according to their magnitude of non-redundant discriminatory power. It does not necessarily provide a ranking of absolute information content; for example, a variable that is highly redundant with a previously selected variable will be ranked low because it possesses little new discriminating information that is not already available to the function. Table 2 shows the order of entry of the training sample variables into the stepwise model with respect to the nine vegetation/land-cover classes.

A variable from each of the three data sets comprises the first three rankings (MLA band 2, SAR ASM, DEM). This immediately confirms that there is discriminatory power available from the three different data sources. The high ranking of texture variables

(SAR ASM and MLA entropy) and geomorphometric variables (slope and incidence) also indicates that additional discriminatory power is provided by image processing. In the case of SAR, the ASM texture variable possessed more relative information than SAR tone. The expected high information content of MLA data with respect to vegetation communities and land-cover classes is confirmed by the first-place ranking of band 2 and the occupation of three of the first five positions by MLA tone and texture variables.

The difference in information content between MLA band 2 (visible) and band 3 (infrared) is shown by their high rankings (first and fifth, respectively). The twelfth-place ranking of MLA band 1 (visible) indicates significant overlap in information content within the visible portion of the spectrum.

The fundamental importance of elevation in explaining class distribution is substantiated by its third-place ranking, while the first-order vertical and horizontal derivatives are seeded near the top half of the available positions. It is interesting that the last three variables entered are all higher-order topographic derivatives. The convexity measures possess little discriminatory information, probably because those physical attributes of the surface have local significance only, but are measured over large areas, producing a variable that appears as random noise essentially. The high level of redundancy between relief and slope (bivariate correlation coefficient = 0.98, table not shown) accounts for the relief measure being ranked last.

Classification Improvements from Image Texture Processing

For each set of variables (see Table 3), a discriminant function was created using the training sample data, and was applied to the test sample to obtain individual and overall class accuracies. Each function variable is assigned a two-letter label; these labels are concatenated into function names in order to reference each combination of variables considered.

Table 4 contains classification results for the functions used to test the first hypothesis, that new variables created by image texture processing will increase individual and overall class accuracies. The MLA image has an overall or average classification accuracy of 73.2 percent, which increases to 87.8 percent when MLA texture is introduced (function MIMT). The average accuracy of 68.7 percent for MLA texture features alone (function MT) suggests that patterns related to the vegetation/land-cover classes are captured adequately in spatial co-occurrence matrices.

Overall classification accuracy for the SAR image is 35.8 percent; this increases to 42.6 percent when SAR texture alone is considered, and to 47.2 percent using SAR tone and texture together (functions ST and SIST, respectively). Although the best result using the SAR is less than 50 percent accurate, the net increase of 11 percent with texture and the fact that texture alone has a higher accuracy than tone illustrates the additional information that exists as textural patterns over the 6-m resolution SAR image. This also supports the notion that relative textural information content increases with finer spatial resolutions (Haralick *et al.*, 1973).

Table 2. Stepwise Discriminant Analysis Order of Entry

Step	Variable Entered
1	MLA Band 2
2	SAR ASM
3	Elevation
4	MLA Entropy
5	MLA Band 3
6	SAR
7	Slope
8	MLA IDM
9	Incidence
10	SAR Entropy
11	MLA ASM
12	MLA Band 1
13	SAR IDM
14	Down Slope Convexity
15	Cross Slope Convexity
16	Relief

Table 3. Discriminant Functions

Function Variables	Number of Variables	Function Name
MLA Image (Band 1,2,3)	3	MI
MLA Image Texture	3	MT
MLA Image and MLA Texture	6	MIMT
SAR Image	1	SI
SAR Image Texture	3	ST
SAR Image and SAR Texture	4	SIST
Digital Elevation Model	1	EL
General System of Geomorphometry	6	GE
MLA Image and the DEM	4	MIEL
MLA Image and Geomorphometry	9	MIGE
MLA Image, MLA Texture and the DEM	7	MIMTEL
MLA Image, MLA Texture and Geomorphometry	12	MIMTGE
SAR Image and the DEM	2	SIEL
SAR Image and Geomorphometry	7	SIGE
SAR Image, SAR Texture and Geomorphometry	10	SISTGE
MLA Image and the SAR Image	4	MISI
MLA Image, MLA Texture, SAR Image, SAR Texture	10	MIMTSIST
Top Three Variables from Stepwise Analysis	3	T3
Top Four Variables from Stepwise Analysis	4	T4
Top Five Variables from Stepwise Analysis	5	T5
All Available Variables	16	ALL

Table 4. Classification Accuracy by Class

Function	Percent Classified into Class									
	1	2	3	4	5	6	7	8	9	$\bar{x}$
MI	89	88	100	99	55	85	38	44	61	**73.2**
MT	70	86	100	98	85	45	19	48	67	**68.7**
MIMT	98	98	100	100	90	89	55	83	77	**87.8**
SI	6	75	96	0	15	48	0	82	0	**35.8**
ST	45	25	100	33	13	4	0	88	75	**42.6**
SIST	56	26	100	31	14	10	2	92	94	**47.2**
EL	75	2	47	100	98	80	61	62	7	**59.1**
GE	71	35	77	100	73	62	84	84	32	**68.7**
MIEL	94	91	100	100	91	88	92	83	92	**92.3**
MIGE	96	88	100	100	94	89	100	93	88	**94.2**
MIMTEL	96	98	100	100	97	95	100	88	88	**95.8**
MIMTGE	97	100	100	100	99	94	100	98	90	**97.6**
SIEL	32	56	98	100	97	70	70	93	29	**71.7**
SIGE	85	40	99	100	83	61	90	93	44	**77.2**
SISTGE	91	38	100	100	87	44	92	97	98	**83.0**
MISI	90	87	100	99	66	87	42	82	48	**77.9**
MIMTSIST	100	99	100	100	92	73	54	98	98	**90.4**
T3	97	79	100	100	98	25	73	100	99	**85.7**
T4	100	99	100	100	99	46	92	100	99	**92.8**
T5	98	100	100	100	99	61	99	100	99	**95.1**
ALL	98	100	100	100	100	89	100	100	99	**98.4**

Individual class accuracies vary within the MLA and SAR data sets according to the spatial arrangement and internal homogeneity of vegetation communities and land-cover classes (that is, some of the classes are dominated by tone, while others are textural in nature). In general, classes that are homogeneous on the ground are characterized best with tone, but those classes which contain unique variability related to land-cover patterns or structural features are discriminated significantly better using image texture. For example, classes 5 (spruce shrub plateau) and 9 (mixed forest) are increased in accuracy by 35 percent (MLA) and 94 percent (SAR) when image texture is used with tone (functions MIMT and SIST, respectively). Similarly, the balsam fir and white birch classes (7 and 8, respectively) increase in accuracy using MLA image texture. These improvements are a result of the unique vegetation patterns and structural (slope/aspect) orientations associated with each class. Conversely, classes 2 (heath barrens) and 6 (black spruce forest) possess internal homogeneity on the ground and show little increase with MLA texture, and decreases in accuracy with SAR texture. This is consistent with ground observations that within-class patterns are either not present or are meaningless in these classes. Therefore, they are best classified using image tone only.

Geomorphometric processing of the DEM results in an overall increase in accuracy from 59.1 percent (function EL) to 68.7 percent (function GE), and increases of 30 percent for class 3 (water), 23 percent for class 7, and 22 percent for class 8. The increases for the balsam fir and white birch forest classes are expected. These classes are controlled topographically by the frontal slopes of Gros Morne Mountain and the steep fiord cliffs near Ten Mile Pond (see Plate 1 and Figures 4 and 5). The water class occurs at different elevations but necessarily has unique geomorphometric derivatives that characterize a flat surface (i.e., zero slope and curvature, undefined aspect).

Despite the marked increases in overall and individual class accuracies possible through image texture processing, it is important to note that the best results achieved are still relatively low in certain instances (e.g., classes 7 and 9 using MLA data; all but classes 3, 8, and 9 with SAR; and classes 2, 6, and 9 with the DEM). This indicates a need for additional information that is not contained in one data source only. As Jones *et al.* (1988) discussed, the classification of vegetation communities may never be satisfactory using spectral data alone. The solution to this — the integration of ancillary data — is evaluated in the next section.

Classification Improvements from Data Integration

Table 4 also contains the results of linear discriminant analyses when the MLA, SAR, and DEM data sets are integrated in various combinations to test the second hypothesis that ancillary information sources provide new information that will improve the discrimination of ground classes. When elevation is used with the three MLA bands (function MIEL), each class increases in accuracy with the greatest increases of between 30 percent and 50 percent found in classes 5, 7, 8, and 9. Each of these forest classes occur on Long Range frontal slopes where a strong elevational control on vegetation communities has been observed. The overall improvement from 73.2 percent (function MI) to 92.3 percent (function MIEL) is comparable to the 87.8 percent accuracy achieved with MLA texture (function MIMT). This supports the earlier interpretation that information related to topographic controls is extracted through image texture processing, and may also suggest that texture can be more important than tone for separating structurally unique classes.

The highest accuracy using MLA and topographic data is achieved through both ancillary data integration and image processing. Overall accuracy is increased to 97.6 percent (function MIMTGE), which is exceeded only when all 16 available MLA, SAR, and DEM variables are used (function ALL: 98.4 percent). The most notable individual class improvement is found in class 8 (white birch forest). The class accuracy is 44 percent using the MLA image alone; this increases to 83 percent with both MLA image texture, and MLA with elevation (functions MIMT and MIEL, respectively). When the image processing and ancillary data integration strategies are combined (function MIMTGE), the highest accuracy (98 percent) is achieved for this class. These deciduous stands are a good example of a class possessing complex surface patterns related to unique topographic form and spatial heterogeneity that are captured separately by both image texture and geomorphometry. All other classes experience similar (but less dramatic) increases using separate image processing and ancillary data integration strategies, with the highest accuracies obtained through a combination of both approaches.

The same trends hold for the SAR data, although the best individual and overall class accuracies achieved are lower than those found when using integrated and processed MLA and DEM data (functions MIMT and MIMTGE). Overall classification accuracy increases from 35.8 percent (SAR alone) to 71.7 percent when the DEM is included (function SIEL). All but one class show moderate (10 percent to 30 percent) to large (in excess of 70 percent) increases in accuracy. Evidence that ancillary elevation is a critical discriminatory information source is both obvious and strong. The only exception is the heath barrens class (2), which decreases in accuracy when elevation and geomorphometry are introduced (functions SIEL and SIGE). This may suggest that topography is not important for this class. It may also be caused in part by the sensitivity of the SAR sensor to the surface moisture content (Wang *et al.*, 1989) present in the high water table, marshes, and open water of this class. The SAR information alone may be sufficient to discriminate this class.

The highest accuracies with SAR data are achieved using both image processing and ancillary data integration. SAR tone with texture and geomorphometry (function SISTGE) yields an overall classification accuracy of 83 percent, with significant class improvements ranging from 20 percent to 70 percent for classes 1, 7, and 9. However, some classes remain below the minimum mapping accuracy level of 85 percent required for most resource management applications (Townshend, 1981). Although different or more sophisticated techniques may increase the accuracy of this classification, the radar image has less information content than the MLA image for the complex terrain and extreme environmental gradients present in the study area. Better results may have been possible had the SAR image been acquired with HV cross polarization (Leckie, 1984).

It was also noted that classes 2 and 6 were classified more accurately with SAR and elevation tone compared to SAR with texture and geomorphometry (functions SIEL and SISTGE, respectively). If suitable knowledge of the spatial patterns and internal homogeneity for such classes exists prior to classification (e.g., from field work, aerial photointerpretation, etc.), it may be possible to devise a two-stage classification approach. In the first stage, classes expected to be characterized adequately (or better) by image tone only would be classified. The appropriate processing algorithms (e.g., texture, geomorphometry) would then be applied to the unclassified portion of the image. Training area statistics for the remaining classes would be generated and the second stage of the classification completed based on a full set of variables. This approach would curtail the use of expensive algorithms (e.g., spatial co-occurrence) and could result in higher overall classification accuracies. For example, if classes 2, 6, and 8 were discriminated by tone (function SIEL) in the first stage, and the remaining pixels by tone, texture, and geomorphometry (function SISTGE) in the second stage, overall classification accuracy could rise to approximately 88 percent. This expectation

is based on individual class accuracies generated by the two functions independently – results may differ with a combined sample or by classification technique.

Integration of the MLA and SAR imagery (function MISI) results in a higher overall classification accuracy (77.9 percent) than use of either image alone. The largest individual class improvement when the SAR is considered as ancillary data is 11 percent for class 5 (spruce shrub plateau). However, the importance of image processing and integration is illustrated by the overall increase from 77.9 percent (function MISI) to 90.4 percent (function MIMTSIST), and by significant individual class accuracy increases ranging from 10 percent to 50 percent. This confirms earlier observations (Franklin and Peddle, 1989; 1990) that additional information content is provided by image texture. However, the MLA and SAR accuracies (function MIMTSIST) are still generally less than those obtained with the full complement of MLA and topographic variables (function MIMTGE), indicating that the DEM is the superior ancillary data source. Recent research (Cooper *et al.*, 1985; Swann *et al.*, 1988) has shown that a DEM can be derived from stereo SPOT MLA data; it may be that an additional spectral data processing step – the creation of the DEM – is needed in classification of mountainous areas.

Finally, several of the highest ranking variables from the stepwise discriminant procedure were entered into the linear discriminant analysis (see Table 2). The top three variables (MLA band 2, SAR ASM, and elevation) had an overall classification accuracy of 85.7 percent (function T3); this increased to 92.8 percent with MLA entropy (T4), and to 95.1 percent when MLA band 3 was added (T5). These represent high classification accuracies that are possible from a relatively small number of variables (compared to, for example, the 12 variables used to obtain 97.6 percent accuracy in function MIMTGE). As ancillary data integration becomes more common and the number of available data channels being considered increases, the *a priori* ranking of variables to determine the best subset of variables in terms of their relative discriminatory power before classification should be considered, especially if (1) training data are limited; (2) the classifier is not robust; (3) data compression techniques (e.g., principal components analysis, canonical correlation vectors) are not available; or (4) computer resources are inadequate or processing times become prohibitive.

CONCLUSIONS

Comparative results of data analyses and image classifications involving high resolution MLA and airborne SAR imagery processed for texture and integrated with ancillary DEM data processed for geomorphometry have been presented for a moderate relief, boreal environment in eastern Canada. Classification accuracies in excess of 90 percent were achieved through a combined image processing/integration strategy for nine landcover classes identified through field work and aerial photointerpretation and which are important in Park management.

Stepwise discriminant analysis revealed that MLA band 2, SAR texture and the DEM possessed the highest relative information content. Linear discriminant functions generated for different variable combinations indicated a need to integrate ancillary DEM information processed for geomorphometry to achieve acceptable class accuracies. For example, the overall accuracy using MLA imagery increased from 73.2 percent to 97.6 percent, and the SAR results increased from 35.8 percent to 83 percent. Such results may be optimized by *a priori* rank analysis and selective image processing to reduce the required number of variables and the processor time, and to avoid problems with classifier robustness.

The next step in this research is to classify more complex ground phenomena, such as natural geomorphic hazard classes that result from processes such as degradation and melting of permafrost in Arctic environments. It is anticipated that such an objective will require even more sophisticated approaches to digital image analysis, including the implementation of a new algorithm to incorporate shape analysis. More powerful classification approaches (e.g., evidential reasoning, context processing, artificial intelligence, and expert systems) will also be necessary in order to achieve a higher level of image understanding.

ACKNOWLEDGMENTS

This research was supported by a Parks Canada contract to NORDCO Limited, St. John's, Newfoundland and NSERC fellowships to Dr. Franklin. Logistical support in the field provided by Mr. Paul Caines, Chief Park Warden Gros Morne National Park, is gratefully acknowledged. The SAR image was acquired through the Canadian Radar Data Development Program and in cooperation with Dr. Charles Livingstone. Mr. Lawrence Davis digitized the elevation model. SPOT data are copywrite, CNES.

REFERENCES

AAACL, 1975. *Biophysical Resources Inventory of Gros Morne National Park*, Airphoto Analysis Associates Co. Ltd., GM Contract Reports 72-89, 73-21, 73-285, Rocky Harbour Newfoundland.

Cooley, W. W., and P. R. Lohnes, 1971. *Multivariate Data Analysis*, John Wiley and Sons: New York.

Cook, E. A., L. R. Iverson, and R. L. Graham, 1989. Estimating Forest Productivity with Thematic Mapper and Biogeographical Data. *Remote Sensing of Environment*. Vol. 28, p. 131–141.

Cooper, P. R., D. E. Friedman, and S. A. Wood, 1985. The Automatic Generation of Digital Terrain Models from Satellite Images by Stereo. *Proceedings of the 36th International Astronautical Congress*. 10 p.

Cross, A. M., D. C. Mason, and S. J. Dury, 1988. Segmentation of Remotely Sensed Images by a Split and Merge Process. *International Journal of Remote Sensing*. Vol. 9, No. 8, pp. 1329–1345.

Curran, P. J., 1985. *Principles of Remote Sensing*. Longman Inc., New York. 282 p.

Davis, J. C., 1987. Contour Mapping and Surface II. *Science*. Vol. 237, pp. 669–672.

Evans, I. S., 1972. General Geomorphometry, Derivatives of Altitude and Descriptive Statistics. *Spatial Analysis in Geomorphology* (R. J. Chorley, ed.): Methuen, London, pp. 17–90.

Fleming, M. D., and R. M. Hoffer, 1979. Machine Processing of Landsat MSS and DMA Topographic Data for Forest Cover Type Mapping. In, *Proceedings of the Fifth Annual Symposium on Machine Processing of Remotely Sensed Data*, LARS, Purdue University, pp. 377–390.

Frank, T. D., 1988. Mapping Dominant Vegetation Communities in the Colorado Rocky Mountain Front Range with Landsat Thematic and Digital Terrain Data. *Photogrammetric Engineering & Remote Sensing*. Vol. 54, No. 12, pp. 1727–1734.

Franklin, S. E., 1987. Terrain Analysis from Digital Patterns in Geomorphometry and Landsat MSS Spectral Response. *Photogrammetric Engineering & Remote Sensing*. Vol. 53, No. 1, pp. 59–65.

———, 1989. Ancillary Data Input to Satellite Remote Sensing of Complex Terrain Phenomena. *Computers & Geosciences*, Vol. 15, No. 5, pp. 799–808.

Franklin, S. E., and D. R. Peddle, 1987. Texture Analysis of Digital Image Data using Spatial Co-occurrence. *Computers & Geosciences*, Vol. 13, No. 3, pp. 293–311.

———, 1989. Spectral Texture for Improved Class Discrimination in Complex Terrain. *International Journal of Remote Sensing*. Vol. 10, No. 8, pp. 1437–1443.

———, 1990. Classification of SPOT HRV Imagery and Texture Features. *International Journal of Remote Sensing*. Vol. 11, No. 3, pp. 551–556.

Franklin, S. E., D. R. Peddle, and J. E. Moulton, 1989. Spectral/Geomorphometric Discrimination and Mapping of Terrain: A Study in Gros Morne National Park. *Canadian Journal of Remote Sensing*. Vol. 15, No. 1, pp. 28–42.

Gersen, D. J., and A. Rosenfeld, 1975. Automatic Sea Ice Detection in

Satellite Pictures. *Remote Sensing of Environment*, Vol. 4, pp. 187–198.

Gordon, D. K., and W. R. Philipson, 1986. A Texture Enhancement Procedure for Separating Orchard from Forest in Thematic Mapper Data. *International Journal of Remote Sensing*. Vol. 8, No. 7, pp. 301–304.

Haralick, R. M., 1979. Statistical and Structural Approaches to Texture. *Proceedings of the IEEE*, Vol. 67, No. 5, pp. 786–804.

Haralick, R. M., K. Shanmugam, and I. Dinstein, 1973. Textural Features for Image Classification: *IEEE Transactions on Systems, Man and Cybernetics*. Vol. 3, No. 6, pp. 610–621.

Hussey, K. J., J. R. Hall, and R. A. Mortensen, 1986. Image Processing Methods in Two and Three Dimensions Used to Animate Remotely Sensed Data. *Proceedings, International Geoscience and Remote Sensing Symposium*, Zurich, Switzerland, pp. 771–776.

Hutchinson, C. F., 1982. Techniques for Combining Landsat and Ancillary Data for Digital Classification Improvement. *Photogrammetric Engineering & Remote Sensing*. Vol. 48, No. 1, pp. 123–130.

Jones, A. R., J. J. Settle, and B. K. Wyatt, 1988. Use of Digital Terrain Data in the Interpretation of SPOT-1 HRV Multispectral Imagery. *International Journal of Remote Sensing*. Vol. 9, No. 4, pp. 669–682.

Kenk, E., and B. Yee, 1988. Methods for Improving the Accuracy of Thematic Mapper Ground Cover Classifications. *Canadian Journal of Remote Sensing*. Vol. 14, No. 1, pp. 17–31.

Klecka, W. R., 1980. *Discriminant Analysis*, Sage University Paper Series on Quantitative Applications in the Social Sciences, 07-019. Sage Publications: Beverly Hills.

Leckie, D. G., 1984. Preliminary Results of an Examination of C-Band Synthetic Aperture Radar for Forestry Applications. *Proceedings, Eighth Canadian Symposium on Remote Sensing*, Montreal, Canada. pp. 151–164.

Lowry, R. T., P. Van Eck, and R. V. Dams, 1986. SAR Imagery for Forestry Management. *Procedings, International Geoscience and Remote Sensing Symposium*, Zurich, Switzerland, pp. 901–906.

Peddle, D. R., 1989. Context Processing of Terrestrial and Oceanic SAR Imagery. *Proceedings, International Geoscience and Remote Sensing/Twelfth Canadian Symposium on Remote Sensing*, Vancouver, Canada. Vol. 5, pp. 2795–2798.

Peddle, D. R., and S. E. Franklin, 1990. GEDEMON: A Fortran-77 Program for Restoration and Derivative Processing of Digital Image Data. *Computers & Geosciences* Vol. 16, No. 5, pp. 669–696.

Pultz, T. J., and R. J. Brown, 1987. SAR Image Classification of Agricultural Targets using First and Second Order Statistics. *Canadian Journal of Remote Sensing*. Vol. 13, No. 2, pp. 85–91.

SAS Institute Inc., 1985. SAS *User's Guide:* Statistics, Cary, North Carolina, 584 p.

Saxon, E. C., 1984. Multitemporal Texture Transformed Landsat Imagery for Mapping Ecological Gradients. *Proceedings of the Third Australasian Remote Sensing Conference*, Brisbane, Australia. pp. 255–259.

Shih, E., and R. Schowengerdt, 1983. Classification of Arid Geomorphic Surfaces using Landsat Spectral and Textural Features. *Photogrammetric Engineering & Remote Sensing*. Vol. 49, No. 3, pp. 337–347.

Skidmore, A. K., 1989. Unsupervised Training Area Selection in Forests using a Nonparametric Distance Measure and Spatial Information. *International Journal of Remote Sensing*. Vol. 10, No. 1, pp. 133–146.

Swain, P. H., and S. M. Davis, 1978. *Remote Sensing, the Quantitative Approach*, McGraw Hill: New York.

Swann, R., D. Hawkins, A. Westwell-Roper, and W. Johnstone, 1988. The Potential of Automated Mapping from Geocoded Digital Image Data. *Photogrammetric Engineering & Remote Sensing*. Vol. 54, No. 2, pp. 187–193.

Teillet, P. M., B. Guindon, J. F. Meunier, and D. G. Goodenough, 1985. Slope Aspect Effects in Synthetic Aperture Radar Imagery. *Canadian Journal of Remote Sensing*. Vol. 11, No. 1, pp. 39–49.

Tom, C. H., and L. D. Miller, 1984. An Automated Land-use Mapping Comparison of the Bayesian Maximum Likelihood and Linear Discriminant Analysis Algorithms. *Photogrammetric Engineering & Remote Sensing*, Vol. 50, No. 2, pp. 193–207.

Townshend, J. R. G., ed.,1981. *Terrain Analysis and Remote Sensing*. George Allen and Unwin: London, 272 p.

Ulaby, F. T., F. Kouyate, B. Brisco, and T. H. L. Williams, 1986. Textural Information in SAR Images. *IEEE Transactions on Geoscience and Remote Sensing*. Vol. GE-24, No. 2, pp. 235–245.

Wang, J. R., J. C. Shuie, T. J. Schmugge, and E. T. Engman, 1989. Mapping Surface Soil Moisture with L-Band Radiometric Measurements. *Remote Sensing of Environment*. Vol. 27, pp. 305–312.

Weszka, J. S., C. R. Dyer, and A. Rosenfeld, 1976. A Comparative Study of Texture Measures for Terrain Classification. *IEEE Transactions on Systems, Man and Cybernetics*. Vol. 10, pp. 269–285.

(Received 7 February 1990; revised and accepted 6 July 1990)

43rd Photogrammetric Week
Stuttgart, 9-14 September 1991

This internationally-recognized "vacation course in photogrammetry" has been held at Stuttgart University since 1973. Because Professor Dr.-Ing. Friedrich Ackermann, one of those responsible for the scientific program, is to retire soon, this 43rd Photogrammetric Week will be his farewell seminar. Essential lines of his work have been chosen as the main topics for the meeting:

• **GPS for Photogrammetry** • **Digital Photogrammetric Image Processing** • **Photogrammetry and Geo-Information Systems** •

Lectures and discussions will be held in the mornings. Technical interpreters will be available for simultaneous translations into German or English. Demonstrations are scheduled for the afternoons.

For further information and applications, contact: Universitat Stuttgart, Institut fur Photogrammetrie, Keplerstrasse 11, D-7000 Stuttgart 1, FRG, telephone 0711/121-3386 or FAX 0711/121-3500.